Fate of classical solitons in one-dimensional quantum systems

M. Pustilnik[1] and K. A. Matveev[2]
[1]*School of Physics, Georgia Institute of Technology, Atlanta, Georgia 30332, USA*
[2]*Materials Science Division, Argonne National Laboratory, Argonne, Illinois 60439, USA*
(Received 19 July 2015; published 23 November 2015)

We study one-dimensional quantum systems near the classical limit described by the Korteweg–de Vries (KdV) equation. The excitations near this limit are the well-known solitons and phonons. The classical description breaks down at long wavelengths, where quantum effects become dominant. Focusing on the spectra of the elementary excitations, we describe analytically the entire classical-to-quantum crossover. We show that the ultimate quantum fate of the classical KdV excitations is to become fermionic particles and holes. We discuss in detail two exactly solvable models exhibiting such crossover, namely the Lieb-Liniger model of bosons with weak contact repulsion and the quantum Toda model. We argue that the results obtained for these models are universally applicable to all quantum one-dimensional systems with a well-defined classical limit described by the KdV equation.

DOI: 10.1103/PhysRevB.92.195146 PACS number(s): 71.10.Pm, 67.10.−j

I. INTRODUCTION

The Korteweg–de Vries (KdV) equation [1] describes propagation of waves in a medium with competing dispersion and nonlinearity and is ubiquitous in the physics of classical nonlinear systems [2]. In addition to the usual periodic waves, the KdV equation supports solitons, i.e., localized disturbances with particlelike properties. Protected by the integrability of the KdV equation, the solitons move and scatter off each other without distortion.

Real systems are never integrable. Nevertheless, the KdV equation often provides an adequate effective description of the excitations in the long-wavelength limit, whereas deviations from the integrability have a significant impact on the lifetime and stability of solitons at shorter wavelengths [3]. Another limitation on the applicability of the KdV equation, which is the primary focus of this paper, arises in one-dimensional quantum systems with a well-defined classical limit. In these systems, quantum effects inevitably become dominant at sufficiently long wavelengths, leading to the breakdown [4–10] of the classical description.

Because the emergence of quantum behavior is not associated with broken integrability, it is natural to approach the problem of describing the classical-to-quantum crossover from the perspective of exactly solvable models [11,12]. Fortunately, solvable models exhibiting such crossover are available. In this paper, we consider two well-known examples. The first one is the Lieb-Liniger model of bosons with weak contact repulsion [11–14]. In the classical limit, its dynamics can be described by the mean-field Gross-Pitaevskii equation [15,16], which has the form of the nonlinear Schrödinger equation [2]. The equation is integrable [2] and reduces to the KdV equation in the long-wavelength limit [17]. The second model we consider is the quantum Toda model [12,18–20]. Its classical counterpart, the Toda model [21], is also integrable and the corresponding equation of motion in the continuum limit coincides [21] with the KdV equation.

It is well known that at high momenta the exact spectra of elementary excitations of the Lieb-Liniger and the quantum Toda models match those deduced from their classical analogs [12,18,22]. In this paper we focus on low momenta, and we evaluate the spectra near the classical-to-quantum crossover. Some of the results presented below have been reported in Refs. [8,9].

The rest of the paper is organized as follows: In Sec. II we summarize some well-known facts about the KdV equation and discuss its applicability for the description of quantum interacting systems near the classical limit. In Sec. III we introduce the Lieb-Liniger and the quantum Toda models and discuss their relation to the KdV equation. Spectra of the elementary excitations are evaluated in Sec. IV. The results are discussed in Sec. V. Technical details are relegated to the Appendixes.

II. KdV EQUATION IN QUANTUM SYSTEMS

The KdV equation in the standard form reads [2]

$$\partial_\tau f + 6 f \partial_\xi f + \partial_\xi^3 f = 0, \tag{2.1}$$

where τ and ξ are the dimensionless time and coordinate, respectively. The equation can be viewed [2] as a canonical equation of motion $\partial_\tau f = \{f,\mathcal{H}\}$ generated by the Hamiltonian

$$\mathcal{H} = \int d\xi \left[f^3 - \frac{1}{2}(\partial_\xi f)^2 \right] \tag{2.2}$$

and the Poisson bracket

$$\{f(\xi), f(\xi')\} = -\partial_\xi \delta(\xi - \xi'). \tag{2.3}$$

The KdV equation supports an infinite number of polynomial integrals of motion [2], all in involution with each other with respect to the Poisson bracket (2.3). Among these integrals of motion are the dimensionless momentum

$$\mathcal{P} = \int d\xi \; f^2 \tag{2.4}$$

and the Hamiltonian (2.2) itself; the latter defines the dimensionless energy. Substituting the single-soliton solution [2] of Eq. (2.1),

$$f_0(\xi,\tau) = \frac{2\mathcal{A}^2}{\cosh^2[\mathcal{A}(\xi - 4\mathcal{A}^2\tau)]}, \tag{2.5}$$

into Eqs. (2.2) and (2.4) and excluding the parameter $\mathcal{A}$, we obtain the relation

$$\mathcal{H}_0 = \frac{1}{5}\left(\frac{3\mathcal{P}_0}{2}\right)^{5/3} \tag{2.6}$$

between the corresponding values of the dimensionless energy and momentum.

In this paper, we study one-dimensional interacting quantum systems with a well-defined classical limit described by the KdV equation. As we will demonstrate in Sec. III, in these systems the low-energy right- and left-moving excitations decouple from each other. Focusing on this regime and on, say, the right-moving excitations, we introduce a bosonic field Φ obeying the commutation relation

$$[\Phi(x),\Phi(y)] = i\pi\,\mathrm{sgn}(x-y) \tag{2.7}$$

and write the Hamiltonian of the right-movers as a sum of two contributions,

$$H = vP + H_{\mathrm{KdV}}, \tag{2.8}$$

where

$$P = \frac{\hbar}{4\pi}\int_0^L dx : (\partial_x\Phi)^2 : \tag{2.9}$$

is the momentum operator and

$$H_{\mathrm{KdV}} = \frac{\hbar^2}{12\pi m_*}\int_0^L dx : \left[(\partial_x\Phi)^3 - a_*^2\left(\partial_x^2\Phi\right)^2\right] : \tag{2.10}$$

represents the leading perturbation. In Eqs. (2.9) and (2.10), L is the size of the system, and the colons denote the normal ordering with respect to the bosonic vacuum. The parameters v, m_*, and a_* have the units of velocity, mass, and length, respectively; their origin and physical meaning will be elucidated below. We are interested in the excitations of the Hamiltonian (2.8) with wavelengths of order a_*. Provided that the length scale a_* is small compared with L, spectra of such excitations are not sensitive to the precise form of the boundary conditions imposed on the field $\Phi(x)$, which we take to be periodic,

$$\Phi(x) = \Phi(x+L). \tag{2.11}$$

Comparison of Eqs. (2.7), (2.9), and (2.10) with Eqs. (2.3), (2.4), and (2.2), respectively, shows that, apart from rescaling, $\partial_x\Phi$ is merely the quantized version of f. The classical model defined by Eqs. (2.2) and (2.3) and its quantum version [23,24] defined by Eqs. (2.7) and (2.10) represent the so-called first Hamiltonian structure of the KdV equation [2]. The quantum KdV model is believed to be integrable, with the first few integrals of motion having the same form [23] as the corresponding classical expressions. These models should be distinguished from those corresponding to the second Hamiltonian structure, in which both the Hamiltonian and the Poisson bracket have forms different from Eqs. (2.2) and (2.3) [2,24]. Whereas quantum KdV models of the latter type have received much attention [24–27] due to their relevance to conformal field theory [28], the former arise naturally as the low-energy description of one-dimensional interacting quantum systems; see, e.g., Refs. [5,9,10,29,30].

Because the operators P and H_{KdV} commute, the excitation spectrum of the Hamiltonian (2.8) has the form

$$\varepsilon(p) = vp + \varepsilon_{\mathrm{KdV}}(p), \tag{2.12}$$

where ε, p, and $\varepsilon_{\mathrm{KdV}}$ are eigenvalues of the operators H, P, and H_{KdV}, respectively. To find the nonlinear-in-p contribution $\varepsilon_{\mathrm{KdV}}(p)$ in Eq. (2.12), we consider the Heisenberg equation of motion $\partial_t\Phi = i\hbar^{-1}[H_{\mathrm{KdV}},\Phi]$, which after a change of variables

$$x = a_*\xi, \quad t = t_*\tau, \quad t_* = \frac{3m_*a_*^2}{\hbar} \tag{2.13}$$

takes the form

$$\partial_\tau\Phi + \tfrac{3}{2} : (\partial_\xi\Phi)^2 : + \partial_\xi^3\Phi = 0. \tag{2.14}$$

We now differentiate Eq. (2.14) with respect to ξ and treat the field

$$F = \tfrac{1}{2}\,\partial_\xi\Phi \tag{2.15}$$

as a classical variable. Neglecting quantum fluctuations of F amounts to replacing $\langle : F^2 : \rangle$ with $\langle F\rangle^2$ and leads to the KdV equation (2.1) for the expectation value $f = \langle F\rangle$. Solution of this equation satisfying the condition $\int_0^{L/a_*} d\xi\; f(\xi,\tau) = 0$ [see Eqs. (2.11) and (2.15)] can be written as

$$f(\xi,\tau) = -\mathcal{N}_0\frac{a_*}{L} + f_0(\xi,\tau), \tag{2.16}$$

where $\mathcal{N}_0 = \int d\xi\; f_0(\xi,\tau) = 2(3\mathcal{P}_0/2)^{1/3}$ is the dimensionless mass of the soliton [2] and f_0 is given by Eq. (2.5). We now take the expectation values of P and H_{KdV} [see Eqs. (2.9) and (2.10)], neglect quantum fluctuations, and compare the resulting expressions with Eqs. (2.2) and (2.4). In the limit $a_*/L \to 0$, this yields

$$p = \frac{\hbar}{\pi a_*}\mathcal{P}_0, \quad \varepsilon_{\mathrm{KdV}} = \frac{2\hbar}{\pi t_*}\mathcal{H}_0. \tag{2.17}$$

Upon introducing the momentum and energy scales

$$p_* = \frac{3\hbar}{2a_*}, \quad \varepsilon_* = \frac{27}{8}\frac{\hbar_*}{t_*} = \frac{p_*^2}{2m_*}, \tag{2.18}$$

we write the KdV contribution to the spectrum as

$$\varepsilon_{\mathrm{KdV}}(p) = \varepsilon_* e(p/p_*). \tag{2.19}$$

For the soliton excitation, the dimensionless function $e(s)$ in Eq. (2.19) is given by

$$e_{\mathrm{soliton}}(s) = \frac{3}{5}\left(\frac{2\pi}{3}\right)^{2/3} s^{5/3}, \tag{2.20}$$

see Eqs. (2.6) and (2.17).

In addition to the solitons, the KdV equation (2.1) has delocalized solutions describing periodic waves, the cnoidal waves [1]. The energy (2.2) and momentum (2.4) associated with such solutions diverge in the limit of infinite system size unless the waves have vanishingly small amplitude. Accordingly, periodic wave solutions of interest here correspond to the harmonic regime when the nonlinear term in Eq. (2.1) can be neglected. This leads to the relation $\Omega = -Q^3$ between the dimensionless frequency Ω and the wave number Q. In classical mechanics, the energy and momentum of such a wave

are proportional to the square of its amplitude. In quantum mechanics, however, the periodic wave solution corresponds to a phonon with well-defined energy and momentum. Restoring the units, we obtain $\varepsilon_{\rm KdV} = \hbar\Omega/t_*$ and $p = \hbar Q/a_*$. The wave dispersion relation can now be converted to the phonon spectrum. It has the form of Eq. (2.19) with $e(s)$ given by

$$e_{\rm phonon}(s) = -s^3. \tag{2.21}$$

Use of the classical equation of motion for the evaluation of the excitation spectrum relies on the assumption that the quantum uncertainty of the field F is negligible. With the help of Eqs. (2.7) and (2.15), the magnitude of quantum fluctuations of F with the length scale $\Delta_\xi \sim 1/\mathcal{A}$ relevant for a classical soliton [see Eq. (2.5)] can be estimated as $\delta F \sim 1/\Delta_\xi \sim \mathcal{A}$. The condition of applicability of the classical description $\delta F \ll \langle F\rangle \sim \mathcal{A}^2$ then leads to $\mathcal{A} \gg 1$, which translates to $\mathcal{P}_0 \gg 1$ for the dimensionless classical momentum (2.4) and to $p \gg p_*$ in Eq. (2.19) or $s \gg 1$ in Eqs. (2.20) and (2.21).

For excitations with small momenta $p \lesssim p_*$, the quantum fluctuations can no longer be neglected, and Eqs. (2.20) and (2.21) are inapplicable. Fortunately, at $p \to 0$, i.e., deep in the quantum regime, the KdV Hamiltonian (2.10) allows further simplification. Indeed, the second term on the right-hand side of (2.10) has a higher scaling dimension than the first one, hence its effect on long-wavelength excitations reduces to being merely a small perturbation [31]. Neglecting this term and employing the well-known mapping [24,32,33] between bosons and fermions,

$$\Psi(x) = \frac{1}{\sqrt{L}} : e^{i\Phi(x)} :, \tag{2.22}$$

we arrive at the fixed-point Hamiltonian [31]

$$H_{\rm fermion} = \frac{\hbar^2}{2m_*}\int_0^L dx :(\partial_x\Psi)^\dagger(\partial_x\Psi):, \tag{2.23}$$

where the symbols : denote the normal ordering with respect to the fermionic vacuum in which all single-particle states with positive (negative) wave numbers are empty (occupied) [24,32,33]. Application of the identity (2.22) also yields the fermionic representation [24,32,33] of the momentum operator (2.9),

$$P = -i\hbar\int_0^L dx :\Psi^\dagger(x)\partial_x\Psi(x):, \tag{2.24}$$

and the relation [32,33]

$$\partial_x\Phi = 2\pi :\Psi^\dagger(x)\Psi(x):, \tag{2.25}$$

which shows that the field F introduced in Eq. (2.15) above is proportional to the density of the effective fermions.

The boundary condition (2.11) and the relation (2.25) imply that $\delta N = \int_0^L dx :\Psi^\dagger(x)\Psi(x): = 0$. Any eigenstate of δN with $\delta N = 0$ can be viewed as a superposition of the particle- and hole-type elementary excitations. The particle excitation is obtained by promoting a fermion from the Fermi level (which corresponds to the single-particle state with wave number zero) to one of the unoccupied single-particle states, whereas in the hole excitation a fermion is removed from one of the occupied single-particle states and placed at the Fermi level. It is easy to see that such particle and hole excitations are eigenstates of $H_{\rm fermion}$ and P. The corresponding eigenvalues $\varepsilon_{\rm fermion}$ and p obviously satisfy

$$\varepsilon_{\rm fermion}(p) = \pm\frac{p^2}{2m_*}, \tag{2.26}$$

where the $+$ ($-$) sign corresponds to the particle (hole) excitation. This expression can be cast in the form (2.19) with

$$e_{\rm fermion}(s) = \pm s^2. \tag{2.27}$$

Note that Eqs. (2.20), (2.21), and (2.27) yield $|e(s)| \sim 1$ at $s \sim 1$. This observation indicates that the classical-to-quantum crossover at $p \sim p_*$ is the only crossover that takes place in the system.

In view of Eqs. (2.15), (2.16), and (2.25), the classical soliton excitation corresponds to a hump in the fermionic density made up of $\mathcal{N} \sim \mathcal{N}_0 \sim s^{1/3}$ fermions drawn from a uniform background. According to the discussion above, the classical description is applicable as long as $\mathcal{N} \gg 1$. On the contrary, the quantum counterpart of the classical soliton, the particle excitation, has exactly one excited fermion, which can be interpreted as $\mathcal{N} = 1$. Quite naturally, the classical-to-quantum crossover occurs at $\mathcal{N} \sim 1$, i.e., when the discreteness of $\mathcal{N}$ can no longer be ignored.

In the above consideration, we treated a_* in Eq. (2.10) as a positive parameter. In fact, it can have either sign. However, it is easy to see that the operators $H_{\rm KdV}(a_*)$ and $H_{\rm KdV}(-a_*)$ are related by the transformation $\Phi \to -\Phi$, which amounts to the particle-hole transformation $\Psi \to \Psi^\dagger$ for fermions; see Eq. (2.22). Under such particle-hole transformation, $H_{\rm KdV}(-a_*) \to -H_{\rm KdV}(a_*)$ and $P \to P$. Accordingly, the spectra of the elementary excitations of $H_{\rm KdV}(-a_*)$ are related to those of $H_{\rm KdV}(a_*)$ and can be written in the form similar to Eq. (2.19) as

$$\varepsilon_{\rm KdV}(p) = -\varepsilon_* e(p/p_*). \tag{2.28}$$

Note that the particle-hole transformation changes the sign of the fermionic density (2.25). Thus, whereas the solitonic excitation of $H_{\rm KdV}(a_*)$ carries $\mathcal{N} > 0$ fermions and corresponds to a hump in the fermionic density, its particle-hole-transformed twin has $\mathcal{N} < 0$, which amounts to a depression. In the nonlinear optics literature, these two kinds of solitons are often referred to as bright and dark solitons, respectively [34].

III. MODELS

Instead of attempting to evaluate the excitation spectrum of the quantum KdV model (2.10) directly, we rely on well-known solvable models, viz. the Lieb-Liniger model and the quantum Toda model. In this section, we demonstrate that in judiciously chosen scaling limits, the low-energy theories describing these models reduce to that defined by Eqs. (2.7)–(2.10). The reduction hinges on the smallness of the parameter

$$\zeta = \frac{\varepsilon_*}{vp_*} = \frac{p_*}{2m_*v}, \tag{3.1}$$

which characterizes the relative magnitude of the KdV contribution to the excitation spectra [see Eq. (2.12)] evaluated near the classical-to-quantum crossover at $p \sim p_*$. Although the low-energy Hamiltonians for both the Lieb-Liniger and

the quantum Toda models contain nonuniversal contributions absent in Eq. (2.8), below we show that these contributions affect the spectra only in the second order in ζ, and

$$\varepsilon(p) = vp_*[s \pm \zeta e(s) + O(\zeta^2)], \quad s = p/p_*. \tag{3.2}$$

Here the + (−) sign corresponds to the quantum Toda (Lieb-Liniger) model, and $e(s)$ [see Eq. (2.19)] are the dimensionless crossover functions describing the spectra of the quantum KdV model (2.10).

A. Lieb-Liniger model

The Lieb-Liniger model [11,13,14]

$$H = \frac{\hbar^2}{2m}\left\{-\sum_l \frac{\partial^2}{\partial x_l^2} + \sum_{l\neq l'} c\,\delta(x_l - x_{l'})\right\} \tag{3.3}$$

describes bosons with contact interaction. We are interested in the thermodynamic limit when both the number of particles N and the system size L are taken to infinity with their ratio, the mean density $n_0 = N/L$, kept fixed. The interaction strength is characterized by the dimensionless parameter [13] $\gamma = c/n_0$. In the weak repulsion regime considered here, $0 < \gamma \ll 1$. The Hamiltonian (3.3) can also be written in the second-quantized form

$$H = \frac{\hbar^2}{2m}\int dx\,[(\partial_x\psi)^\dagger(\partial_x\psi) + cn^2(x)], \tag{3.4}$$

where $n(x) = \psi^\dagger(x)\psi(x)$ is the density operator. Hereafter, products of quantum fields at the same spatial point, such as $n^2(x)$ in Eq. (3.4), are to be understood as being normal-ordered with respect to the appropriate vacuum states; cf. Sec. II.

We are interested in excitations with wavelengths much longer than the mean interparticle distance $1/n_0$. Following the standard prescription [35,36], we write

$$\psi(x) = \sqrt{n(x)}\,e^{-i\vartheta(x)}. \tag{3.5}$$

Here $n(x)$ is the coarse-grained (averaged over a region much larger than $1/n_0$) particle density, which can be regarded as a continuous function of x, and the field ϑ satisfies [35,36]

$$[n(x),\vartheta(y)] = -i\delta(x-y). \tag{3.6}$$

We will assume that ϑ obeys the periodic boundary condition $\vartheta(x+L) = \vartheta(x)$. This assumption amounts [36] to restricting one's attention to excitations near the zero-momentum ground state.

Substitution of $\psi(x)$ in the form (3.5) into Eq. (3.4) yields

$$H = \frac{\hbar^2}{2m}\int dx\left[n(\partial_x\vartheta)^2 + \frac{1}{4n}(\partial_x n)^2 + cn^2\right]. \tag{3.7}$$

For low-energy excitations, deviations of the density $n(x)$ from its mean value n_0 are small. It is therefore convenient to write $n(x)$ as

$$n(x) = n_0 + \frac{1}{\pi}\partial_x\varphi, \tag{3.8}$$

where the new bosonic field φ satisfies

$$[\partial_x\varphi,\vartheta(y)] = -i\pi\delta(x-y) \tag{3.9}$$

and obeys the periodic boundary condition. Successive approximations for the low-energy Hamiltonian are obtained by substituting Eq. (3.8) into Eq. (3.7) and expanding in powers of $\partial_x\varphi$.

The leading contribution to the low-energy Hamiltonian contains operators of scaling dimension 2, and it has the standard Luttinger liquid form [33,35–37]

$$H_0 = \frac{\hbar v}{2\pi}\int dx[K(\partial_x\vartheta)^2 + K^{-1}(\partial_x\varphi)^2]. \tag{3.10}$$

Here

$$v = \frac{\hbar n_0}{m}\sqrt{\gamma}, \quad K = \frac{\pi\hbar n_0}{mv} = \frac{\pi}{\sqrt{\gamma}} \tag{3.11}$$

are the sound velocity and the Luttinger-liquid parameter evaluated in the leading order in $\gamma \ll 1$. Instead of φ and ϑ, it is convenient to introduce the right- and left-moving fields

$$\varphi_\pm(x) = \frac{1}{\sqrt{K}}\,\varphi(x) \mp \sqrt{K}\,\vartheta(x), \tag{3.12}$$

which satisfy $[\partial_x\varphi_+,\varphi_-(y)] = [\varphi_+(x),\partial_y\varphi_-] = 0$ and

$$[\varphi_\pm(x),\varphi_\pm(y)] = \pm i\pi\,\mathrm{sgn}(x-y). \tag{3.13}$$

Writing the Luttinger-liquid Hamiltonian (3.10) in terms of $\varphi_\pm$ reveals its chiral (i.e., diagonal in the basis of the right- and left-movers) structure,

$$H_0 = \frac{\hbar v}{4\pi}\int dx\sum_{v=\pm}(\partial_x\varphi_v)^2. \tag{3.14}$$

In addition to the Hamiltonian, we need the momentum operator $P = -i\hbar\int dx\,\psi^\dagger\partial_x\psi$. Substituting Eq. (3.5) here and taking into account Eq. (3.8), we obtain

$$P = -\hbar\int dx\,n\partial_x\vartheta = -\frac{\hbar}{\pi}\int dx\,(\partial_x\varphi)(\partial_x\vartheta). \tag{3.15}$$

Written in terms of the right- and left-movers $\varphi_\pm$, see Eq. (3.12), the momentum (3.15) takes the form

$$P = P_+ + P_-, \quad P_\pm = \pm\frac{\hbar}{4\pi}\int dx\,(\partial_x\varphi_\pm)^2. \tag{3.16}$$

Comparison of Eqs. (3.14) and (3.16) shows that the Luttinger-liquid Hamiltonian (3.14) can be written as

$$H_0 = v(P_+ - P_-). \tag{3.17}$$

The nonlinear corrections to the excitation spectra arise due to higher-order terms in the gradient expansion of the Hamiltonian (3.7). Collecting the chiral terms with scaling dimensions 3 and 4 in this expansion, we write the resulting contribution in the form of the quantum KdV Hamiltonian (2.10),

$$H_1 = \frac{\hbar^2}{12\pi m_*}\int dx\sum_v\left[(\partial_x\varphi_v)^3 + a_*\left(\partial_x^2\varphi_v\right)^2\right], \tag{3.18}$$

where the effective mass m_* and the emergent length scale a_* are defined by

$$\frac{m}{m_*} = \frac{3}{4\sqrt{K}}, \quad a_*n_0 = \frac{K^{3/2}}{2\pi^2} \tag{3.19}$$

and satisfy $m/m_* \ll 1$, $a_* n_0 \gg 1$. Note that the result for the effective mass agrees with the general expression [5,38]

$$\frac{m}{m_*} = \frac{1}{2v\sqrt{K}} \frac{d(vn_0)}{dn_0}, \tag{3.20}$$

valid for any Galilean-invariant system.

Although the second term in Eq. (3.18) has a higher scaling dimension than the first one, its effect on the excitations with wavelengths of order a_* [or, equivalently, with momenta of order $p_* \sim \hbar/a_*$; see Eq. (2.18)] is comparable with that of the first term in Eq. (3.18). The key observation is that for weakly interacting bosons

$$\frac{p_*}{\hbar n_0} = \frac{3\pi}{K^{3/2}} \ll 1, \tag{3.21}$$

i.e., such excitations belong to the realm of the long-wavelength description based on the gradient expansion. Changing the integration variable in Eqs. (3.14) and (3.18) to $\xi = x/a_*$, we write the expansion $H = H_0 + H_1 + \cdots$ as

$$H = vp_*(h_0 + \zeta h_1 + \zeta h_1' + \zeta^2 h_2 + \cdots), \tag{3.22}$$

with the parameter ζ introduced in Eq. (3.1). Using Eqs. (3.11), (3.19), and (3.21), we find

$$\zeta = \frac{9}{8K} \ll 1. \tag{3.23}$$

The operators h_0 and h_1 in Eq. (3.22) are given by

$$h_0 = \frac{1}{6\pi} \int d\xi \sum_\nu (\partial_\xi \varphi_\nu)^2, \tag{3.24a}$$

$$h_1 = \frac{2}{27\pi} \int d\xi \sum_\nu \left[(\partial_\xi \varphi_\nu)^3 + \left(\partial_\xi^2 \varphi_\nu\right)^2\right], \tag{3.24b}$$

cf. Eqs. (3.14) and (3.18). The third term in Eq. (3.22) includes nonchiral contributions with scaling dimensions 3 and 4 omitted in Eq. (3.24b), $(\partial_\xi \varphi_\pm)^2(\partial_\xi \varphi_\mp)$ and $(\partial_\xi^2 \varphi_+)(\partial_\xi^2 \varphi_-)$. Contributions in Eq. (3.22) that are higher order in ζ originate in the expansion of the second term in Eq. (3.7), the so-called quantum pressure [16], in $\partial_x \varphi$. The first term in this series yields h_2 in Eq. (3.22), which contains operators of scaling dimension 5, $(\partial_\xi^2 \varphi_\nu)^2(\partial_\xi \varphi_\nu)$.

The expansion (3.22) allows us to classify various terms in the low-energy Hamiltonian according to the order of magnitude of their contributions to the energy of chiral excitations. It should be emphasized that this classification is different from the usual notion of scaling dimension. Indeed, the latter is relevant for the description of excitations in the limit of infinitely long wavelengths, whereas we are interested in excitations characterized by long but finite wavelengths of order a_*.

We proceed by singling out the first two terms in the expansion (3.22), $\widetilde{H} = vp_*(h_0 + \zeta h_1)$, treating the remainder of the expansion as a perturbation. Taking into account that $\widetilde{H}$ commutes with $P_\pm$, we consider a simultaneous eigenstate of the operators P_+, P_-, and $\widetilde{H}$ with eigenvalues $p_+ = p \sim p_*$, $p_- = 0$, and $\widetilde{\varepsilon}$, respectively. In the right-moving sector (i.e., when acting on states with $p_- = 0$, such as the one we discuss), the unperturbed Hamiltonian $\widetilde{H}$ coincides with that defined by Eqs. (2.7)–(2.10), with a_* in $H_{\rm KdV}$ [see Eq. (2.10)] replaced with $-a_*$. Using Eqs. (2.12), (2.28), and (3.1), we obtain $\widetilde{\varepsilon}(p) = vp_*[s - \zeta e(s)]$ with $s = p/p_*$.

Perturbation theory in $H - \widetilde{H} = vp_*(\zeta h_1' + \zeta^2 h_2 + \cdots)$ establishes the correspondence between the eigenstate of $\widetilde{H}$ we consider and the eigenstate of the full Hamiltonian H with the energy $\varepsilon = \widetilde{\varepsilon} + \delta\varepsilon$. The latter state is also an eigenstate of the total momentum P [see Eq. (3.16)] with the eigenvalue p. The leading corrections to the energy arise in the second order in h_1' (note that h_1' has zero expectation value in the right-moving eigenstate of $\widetilde{H}$), and in the first order in h_2. Both contributions can be estimated as $\delta\varepsilon \sim vp_*\zeta^2$. Accordingly, $\varepsilon(p) = \widetilde{\varepsilon}(p) + O(vp_*\zeta^2)$, leading to Eq. (3.2).

B. Quantum Toda model

The classical Toda model [21] describes a chain of N particles with exponential nearest-neighbor interaction,

$$H = \sum_l \left[\frac{p_l^2}{2m} + V_0 e^{-2D_l/a_0}\right], \quad D_l = x_{l+1} - x_l. \tag{3.25}$$

We consider a system of size L in the thermodynamic limit taken at a fixed particle density $n_0 = N/L$. The potential energy in Eq. (3.25) is minimized in the ordered configuration $x_1 < x_2 < \cdots < x_N$, in which the distance between neighboring particles D_l equals its mean value $1/n_0$. At finite but sufficiently low energies, the deviations from the mean $\delta D_l = D_l - 1/n_0$ remain small compared with the interaction range a_0. In such a weakly anharmonic regime, the interaction potential in Eq. (3.25) can be expanded in series in $\delta D_l/a_0$. After taking a continuum limit and making an appropriate change of variables, the leading terms of such an expansion can be cast [21] in the form of the KdV Hamiltonian (2.2). The model (3.25) is integrable and supports solitonic excitations with arbitrarily high energies, well beyond the weakly anharmonic regime [21]. However, these excitations, the Toda solitons, can no longer be described in the KdV framework.

In the quantum Toda model [12,18–20], coordinates of the particles x_l and their momenta p_l are replaced with the operators satisfying $[x_l, p_{l'}] = i\hbar\delta_{l,l'}$. Unlike the classical Toda model, the very existence of the weakly anharmonic regime is not *a priori* guaranteed even at low energies but hinges on the smallness of quantum fluctuations of δD_l. The lower bound δD on the magnitude of these fluctuations can be estimated as the amplitude of zero-point oscillations of the positions of the particles near the respective potential minima. It is convenient to characterize the range and the strength of the interaction potential in Eq. (3.25) by the dimensionless parameters

$$\alpha = \frac{1}{a_0 n_0}, \quad \beta = \frac{1}{2\alpha e^\alpha} \frac{\sqrt{mV_0}}{\hbar n_0}. \tag{3.26}$$

In terms of these parameters, $\delta D \sim a_0 \beta^{-1/2}$ and the necessary condition for the existence of the weakly anharmonic regime $\delta D \ll a_0$ translates to

$$\beta \gg 1, \tag{3.27}$$

irrespective of the value of α.

The quantum Toda model is integrable [19,20], and its properties can be studied analytically [20] at arbitrary values

of the parameters α and β. However, our goal is to describe excitations in the universal KdV regime rather than to explore various regimes of the quantum Toda model. Therefore, we make a simplifying assumption

$$\alpha \gg 1. \tag{3.28}$$

The advantage of working in the dilute limit (3.28) is twofold. First, as shown below, in this limit $\zeta \sim 1/\beta$, hence Eq. (3.27) guarantees the existence of the KdV regime. Second, excitations of the Toda model in the dilute limit can be studied [12,18] by considering instead the hyperbolic Calogero-Sutherland model [12,18,39]

$$H = \frac{\hbar^2}{2m}\left\{-\sum_l \frac{\partial^2}{\partial x_l^2} + \sum_{l\neq l'} \frac{\lambda(\lambda-1)}{a_0^2 \sinh^2[(x_l - x_{l'})/a_0]}\right\}. \tag{3.29}$$

For large λ the distance between neighboring particles is close to $1/n_0 \gg a_0$; see Eq. (3.28). Therefore, the sinh function in Eq. (3.29) can be approximated by exponential, and the interaction can be restricted to nearest neighbors. Thus, the model (3.29) is equivalent [12,18] to the Toda model (3.25) with

$$V_0 = \frac{4\hbar^2\lambda(\lambda-1)}{ma_0^2}. \tag{3.30}$$

Substitution into Eq. (3.26) gives

$$\beta = \sqrt{\lambda(\lambda-1)}\, e^{-\alpha} \approx \lambda e^{-\alpha}, \tag{3.31}$$

and the condition Eq. (3.27) yields

$$\lambda \gg e^{\alpha}. \tag{3.32}$$

The inequalities (3.28) and (3.32) define the Toda limit of the hyperbolic Calogero-Sutherland model (3.29). Unlike the quantum Toda model (3.25), the hyperbolic Calogero-Sutherland model (3.29) is solvable by the asymptotic Bethe ansatz [12,18], which allows it to be handled on equal footing with the Lieb-Liniger model.

For long-wavelength excitations, p_l and D_l in Eq. (3.25) vary with l on the scale much larger than unity, and l can be treated as a continuous variable. Replacing the summation over l in Eq. (3.25) with the integration, we write the low-energy Hamiltonian as

$$H = \int dl \left[\frac{p^2(l)}{2m} + V_0 e^{-2D(l)/a_0}\right], \tag{3.33}$$

where $D(l) = x(l+1) - x(l)$, and the fields $x(l)$ and $p(l)$ satisfy $[x(l), p(l')] = i\hbar\delta(l-l')$.

The Hamiltonian (3.33) describes the strongly interacting quantum fluid in terms of the so-called Lagrangian variables [9,40,41], in which the position of the fluid element is specified by l rather than by its physical coordinate $x(l)$. The consideration in Secs. II and III A, however, follows the conventional bosonization scheme [35–37] based on the Eulerian [40,41] description of the quantum fluid. A switch to the Eulerian formulation is accomplished using

$$dl = n(x)dx, \tag{3.34}$$

where $n(x)$ is the coarse-grained density operator, and writing the momentum per particle $p(l)$ as [41]

$$p(l) = -\hbar\partial_x\vartheta, \tag{3.35}$$

where the field ϑ has essentially the same meaning as that in Eq. (3.5) and satisfies the same commutation relation (3.6). Indeed, substituting Eqs. (3.34) and (3.35) into the expression $P = \int dl\, p(l)$, we recover Eq. (3.15) for the momentum operator, $P = -\hbar\int dx\, n(x)\partial_x\vartheta$.

The Eulerian form of the interparticle distance $D(l)$ in Eq. (3.33) follows from the identity $D(l) = [e^{\partial_l} - 1]x(l)$. Replacing ∂_l with $n^{-1}\partial_x$ here [see Eq. (3.34)], we find

$$\begin{aligned} D &= \left(e^{n^{-1}\partial_x} - 1\right)x \\ &= \frac{1}{n} + \frac{1}{2!}\frac{1}{n}\partial_x\frac{1}{n} + \frac{1}{3!}\frac{1}{n}\partial_x\frac{1}{n}\partial_x\frac{1}{n} + \cdots, \end{aligned} \tag{3.36}$$

i.e., D depends on the density $n(x)$ and its derivatives. Predictably, D reduces to $1/n$ in the long-wavelength limit.

Using Eqs. (3.34) and (3.35), we rewrite the Hamiltonian (3.33) as

$$H = \frac{\hbar^2}{2m}\int dx\, n(\partial_x\vartheta)^2 + U[n], \tag{3.37}$$

where the interaction energy $U[n]$ is a functional of density,

$$U[n] = V_0\int dx\, n e^{-2D/a_0} \tag{3.38}$$

with D given by Eq. (3.36). Note that the field ϑ enters the Hamiltonian (3.37) only via the kinetic energy term, which has the same form as that in Eq. (3.7). This is a direct consequence of the Galilean invariance of the models (3.3) and (3.25).

The remaining consideration parallels that in Sec. III A: we write the density $n(x)$ in the form (3.8) and expand the Hamiltonian (3.37) in $\partial_x\varphi$. The leading contribution in this expansion is the Luttinger-liquid Hamiltonian (3.10) with

$$K = \frac{\pi}{4\alpha^2\beta} \ll 1. \tag{3.39}$$

In the next step, we pick terms containing integrals of $(\partial_x\varphi)(\partial_x\vartheta)^2$, $(\partial_x^2\varphi)^2$, and $(\partial_x\varphi)^3$. Expressing φ and ϑ via the right-/left-moving fields $\varphi_\pm$ [see Eq. (3.12)] and omitting all nonchiral terms, we obtain the KdV contribution

$$H_1 = \frac{\hbar^2}{12\pi m_*}\int dx \sum_\nu \left[(\partial_x\varphi_\nu)^3 - a_*\left(\partial_x^2\varphi_\nu\right)^2\right]. \tag{3.40}$$

Except for the sign of the second term on the right-hand side, Eq. (3.40) has the same form as Eq. (3.18). The effective mass m_* and the emergent length scale a_* in Eq. (3.40) are defined by

$$\frac{m}{m_*} = \alpha^2\sqrt{\beta/\pi} = \frac{\alpha}{2\sqrt{K}}, \tag{3.41a}$$

$$a_* n_0 = \frac{1}{2}\sqrt{\pi\beta} = \frac{\pi}{4\alpha\sqrt{K}}, \tag{3.41b}$$

again in agreement with Eq. (3.20). Taking into account Eqs. (3.27) and (3.28), we find $m/m_* \gg 1, a_* n_0 \gg 1$.

Substitution of Eq. (3.41b) into Eq. (2.18) yields

$$\frac{p_*}{\hbar n_0} = \frac{3}{\sqrt{\pi\beta}} = \frac{6\alpha}{\pi}\sqrt{K} \ll 1 \tag{3.42}$$

for the crossover momentum. The expansion parameter ζ [see Eq. (3.1)] is then given by

$$\zeta = \frac{3}{8\pi\beta} = \frac{3}{2\pi^2}\alpha^2 K \ll 1. \tag{3.43}$$

Focusing on excitations with wavelengths of order a_*, we change the integration variable to $\xi = x/a_*$ and write the gradient expansion of the low-energy Hamiltonian in the form (3.22). The Luttinger-liquid contribution in this expansion, h_0, is given by Eq. (3.24a), and the KdV contribution h_1 differs from Eq. (3.24b) only in the sign of the second term on the right-hand side. The remaining terms in the expansion (3.22) are nonuniversal. The third term, h_1', contains nonchiral contributions with scaling dimensions 3 and 4, whereas the fourth term, h_2, is composed of the chiral contributions $(\partial_\xi\varphi_\nu)^4$, $(\partial_\xi\varphi_\nu)^2(\partial_\xi^3\varphi_\nu)$, and $(\partial_\xi^3\varphi_\nu)^2$, which originate in the expansion of the interaction energy Eq. (3.38). Importantly, various operators enter h_1' and h_2 with numerical coefficients that have finite limits of order unity at $\alpha \to \infty$.

Repeating the analysis of Sec. III A, we conclude that h_1' and h_2 contribute to the energy of chiral excitations with momenta $p \sim p_*$ only in the second order in ζ. Therefore, to first order in ζ the excitation spectrum is given by Eqs. (2.12) and (2.19), leading to Eq. (3.2) with a positive sign of the second term on the right-hand side.

IV. ELEMENTARY EXCITATIONS

As shown in Secs. II and III, excitation spectra of the chiral model defined by Eqs. (2.7)–(2.10), the Lieb-Liniger model (3.3), and the quantum Toda model (3.25) are given by Eq. (3.2). The nontrivial parts of the spectra are described by the universal dimensionless crossover functions $e(s)$, with asymptotes given by Eqs. (2.20) and (2.21) in the classical limit $s \gg 1$, and by Eq. (2.27) in the quantum limit $s \ll 1$. In this section, we take advantage of the integrability of the Lieb-Liniger and the hyperbolic Calogero-Sutherland models. We evaluate their spectra to first order in ζ and extract the crossover functions $e(s)$.

A. Excitation spectra from the Bethe ansatz

The Lieb-Liniger model (3.3) and the hyperbolic Calogero-Sutherland model (3.29) are integrable by the Bethe ansatz [[11–14]]: their many-body eigenstates are parametrized by sets of N rapidities $q_1, q_2, \ldots, q_N$, which are similar to the wave numbers of free fermions. Lieb's type I and type II excitations [13] can be viewed as, respectively, particle- and hole-type excitations of the corresponding Fermi sea [11–14]. Their momenta and energies are given parametrically by

$$p(q) = 2\pi\hbar\left|\int_{q_0}^{q} dq'\rho(q')\right|, \quad \varepsilon(q) = \left|\int_{q_0}^{q} dq'\sigma(q')\right|, \tag{4.1}$$

where $q > q_0$ ($q < q_0$) for the type I (type II) excitations, and q_0 is the Fermi rapidity. The function $\rho(q) = L^{-1}\sum_{i=1}^{N}\delta(q - q_i)$ is the density of rapidities in the ground state. In the thermodynamic limit, $\rho(q)$ can be viewed as a continuous function of q, normalized as [11–13]

$$\int_{-q_0}^{q_0} dq\,\rho(q) = n_0, \tag{4.2}$$

and satisfying the Lieb equation [11–13]

$$\rho(q) + \frac{1}{2\pi}\int_{-q_0}^{q_0} dq'\Theta'(q - q')\rho(q') = \frac{1}{2\pi}, \tag{4.3}$$

where $\Theta(q)$ is the two-particle scattering phase shift (see below). The function $\sigma(k)$ in the second equation in (4.1) is the derivative of the energy function introduced in Ref. [14]. It obeys the Yang-Yang equation [11,12,14]

$$\sigma(q) + \frac{1}{2\pi}\int_{-q_0}^{q_0} dq'\Theta'(q - q')\sigma(q') = \frac{\hbar^2 q}{m}. \tag{4.4}$$

The functions $\rho(q)$ and $\sigma(q)$ are, respectively, even and odd functions of their argument [11,12]. Their values at the Fermi rapidity $\rho_0 = \rho(q_0)$ and $\sigma_0 = \sigma(q_0)$ satisfy [11,12]

$$\frac{\sigma_0}{\rho_0} = 2\pi\hbar v, \quad \sigma_0\rho_0 = \frac{\hbar^2 n_0}{2m}. \tag{4.5}$$

Taking into account the relation between the sound velocity v and the Luttinger-liquid parameter K [see Eq. (3.11)], we obtain

$$\rho_0 = \frac{\sqrt{K}}{2\pi}, \quad \sigma_0 = \hbar v\sqrt{K}. \tag{4.6}$$

The two-particle scattering phase shift $\Theta(q)$ in Eqs. (4.3) and (4.4) is given by [11–13]

$$\Theta(q) = -2\arctan(q/c) \tag{4.7}$$

for the Lieb-Liniger model (3.3), and by [12,18]

$$\Theta(q) = 2\,\mathrm{Im}\left[\ln\Gamma\left(\lambda + \frac{ia_0 q}{2}\right) - \ln\Gamma\left(1 + \frac{ia_0 q}{2}\right)\right] \tag{4.8}$$

for the hyperbolic Calogero-Sutherland model (3.29). At $|q| \ll \lambda/a_0$ [for α and λ satisfying Eqs. (3.28) and (3.32), this range includes $|q| \sim q_0$], Eq. (4.8) simplifies to

$$\Theta(q) = a_0 q\ln\lambda - 2\,\mathrm{Im}\ln\Gamma\left(1 + \frac{ia_0 q}{2}\right). \tag{4.9}$$

The approximation (4.9) is adequate for excitations with not too high energies, such as $\varepsilon \sim vp_*$, and it is equivalent [12,18,20] to neglecting the difference between the hyperbolic Calogero-Sutherland model and the quantum Toda model. For brevity, we shall refer to the results obtained in the framework of the approximation (4.9) as pertaining to the quantum Toda model.

The dependence on q in both Eqs. (4.7) and (4.9) is characterized by a single scale q_*, with $q_* = c$ for the Lieb-Liniger model and $q_* = 2/a_0$ for the hyperbolic Calogero-Sutherland model. In the regimes we consider, these scales are small compared with the respective values of the Fermi rapidities,

$$\frac{q_*}{q_0} \sim \zeta \ll 1, \tag{4.10}$$

where ζ is the small parameter introduced in Sec. III; see Eqs. (3.1), (3.23), and (3.43). Moreover, it follows from Eqs. (3.11), (3.21), (3.39), (3.42), and (4.6) that

$$p_* = 6\hbar\rho_0 q_* \tag{4.11}$$

for both models considered. Equations (4.1) then show that $|q - q_0| \sim q_*$ corresponds to $p(q) \sim p_*$ and $\varepsilon(q) \sim vp_*$. Thus, in order to study the excitation spectra at the classical-to-quantum crossover, it is sufficient to find ρ and σ in the vicinity of one of the Fermi rapidities, say, at $q \approx q_0$. Accordingly, it is convenient to work with the "shifted" dimensionless rapidities

$$t = \frac{q - q_0}{q_*} \tag{4.12}$$

instead of q.

In terms of t, the classical-to-quantum crossover at $p \sim p_*$ corresponds to $|t| \sim 1$, which is well within the range $|t| \ll q_0/q_* \sim 1/\zeta$. At such t, the difference between the normalized functions

$$\varrho(t) = \frac{\rho(t)}{\rho_0}, \quad \varsigma(t) = \frac{\sigma(t)}{\sigma_0} \tag{4.13}$$

is very small, of order $\zeta \ll 1$. However, this difference cannot be neglected as it is responsible for the nonlinear corrections to the excitation spectra. Indeed, with the help of Eqs. (4.11)–(4.13), Eqs. (4.1) can be cast in the form

$$\frac{p}{p_*} = \pm\frac{\pi}{3}\int_0^{\pm\tau} dt\, \varrho(t), \tag{4.14a}$$

$$\frac{\varepsilon_\pm - vp}{vp_*} = \pm\frac{\pi}{3}\int_0^{\pm\tau} dt[\varsigma(t) - \varrho(t)], \tag{4.14b}$$

where $0 < \tau \ll 1/\zeta$ and the $+$ $(-)$ signs correspond to the type I (type II) excitation.

B. Crossover functions and their properties

According to the discussion in Secs. II and III, the excitation spectra at $\zeta \to 0$ are given by Eq. (3.2), which we write here as

$$\varepsilon_\pm(p) = vp_*[s + \zeta e_\pm(s) + O(\zeta^2)], \quad s = p/p_*. \tag{4.15}$$

Comparison of Eq. (4.15) with Eqs. (4.14) then yields the dimensionless crossover functions $e_\pm(s)$ in the form

$$e_\pm(s) = \pm E(\pm s), \tag{4.16}$$

where $s > 0$ and the function $E(S)$ is defined parametrically by

$$S(\tau) = \frac{\pi}{3}\int_0^\tau dt\, \varrho_0(t), \quad E(\tau) = \frac{\pi}{3}\int_0^\tau dt\, \eta_0(t). \tag{4.17}$$

Here τ may have either sign, and the functions $\varrho_0(t)$ and $\eta_0(t)$ are given by

$$\varrho_0(t) = \lim_{\zeta\to 0}\varrho(t) = \lim_{\zeta\to 0}\varsigma(t), \tag{4.18a}$$

$$\eta_0(t) = \lim_{\zeta\to 0}\frac{1}{\zeta}[\varsigma(t) - \varrho(t)], \tag{4.18b}$$

with the limits $\zeta \to 0$ evaluated at fixed t.

Further insight is provided by the asymptotic solutions of the Bethe ansatz equations (4.3) and (4.4) at q satisfying $q_* \ll |q - q_0| \ll q_0$, or, equivalently, at t in the range $1 \ll |t| \ll 1/\zeta$; see Eqs. (4.10) and (4.12). As discussed above, this range corresponds to the classical regime in the excitations spectra. Such classical solutions have been found in Refs. [13,22] for the Lieb-Liniger model and in Ref. [18] (see also Ref. [12] for a review) for the quantum Toda model. These solutions and the approximations involved are reviewed in Appendix A. Substituting the classical solutions into Eqs. (4.18), we obtain

$$\varrho_0(t) = \begin{cases} (\pi t)^{-1/2}, & t \gg 1, \\ |4t/\pi|^{1/2}, & -t \gg 1 \end{cases} \tag{4.19}$$

for the Lieb-Liniger model and

$$\varrho_0(t) = \begin{cases} (4t/\pi)^{1/2}, & t \gg 1, \\ |\pi t|^{-1/2}, & -t \gg 1 \end{cases} \tag{4.20}$$

for the quantum Toda model, and the relation

$$\eta_0(t) = \frac{2\pi}{3}\int_0^t dt'\varrho_0(t') = 2S(t), \tag{4.21}$$

valid for both models. The relation (4.21) turns out to be applicable at all t, not only at $|t| \gg 1$. This can be shown rigorously; see Appendix B.

With Eq. (4.21) at hand, the task of evaluating the crossover functions reduces to finding the function $\varrho_0(t)$ introduced in Eq. (4.18a). We therefore turn to the Lieb equation (4.3), divide it by ρ_0 [see Eqs. (4.6) and (4.13)], change the variable according to Eq. (4.12), and write the resulting equation as

$$\varrho(t) + \frac{1}{2\pi}\int_{-2k_0}^0 dt'\Theta'(t - t')\varrho(t') = \frac{1}{2\pi\rho_0}, \tag{4.22}$$

where $k_0 = q_0/q_* \sim 1/\zeta$; see Eq. (4.10).

For the Lieb-Liniger model, the kernel $\Theta'(t)$ in Eq. (4.22) is given by

$$\Theta'(t) = -\frac{2}{1 + t^2}, \tag{4.23}$$

whereas $1/\rho_0 \propto \zeta^{1/2}$. Accordingly, in the limit $\zeta \to 0$, Eq. (4.22) turns into a homogeneous equation,

$$\varrho_0(t) + \frac{1}{2\pi}\int_{-\infty}^0 dt'\Theta'(t - t')\varrho_0(t') = 0. \tag{4.24}$$

Augmented with the condition $\varrho_0(0) = 1$, Eq. (4.24) has a unique solution for the normalized density $\varrho_0(t)$. This solution is derived in Appendix C. At large $|t|$ it agrees with Eq. (4.19), as expected. Note that $\Theta'(t - t')\varrho_0(t')|_{t'\to-\infty} \propto |t'|^{-3/2}$, hence the integral on the left-hand side of Eq. (4.24) converges.

For the quantum Toda model,

$$\Theta'(t) = 2\ln\lambda - 2\,\mathrm{Re}\,\psi(1 + it), \tag{4.25}$$

where $\psi(z) = d\ln\Gamma(z)/dz$ is the digamma function. With Eq. (4.20) taken into account, this gives $\Theta'(t - t')\varrho_0(t')|_{t'\to-\infty} \propto |t'|^{-1/2}\ln|\lambda/t'|$, and the integral in the analog of Eq. (4.24) would be divergent. This difficulty is circumvented by first differentiating Eq. (4.22) with respect to t, and only then taking the limit $\zeta \to 0$. The resulting

integrodifferential equation

$$\varrho_0'(t) + \frac{1}{2\pi}\int_{-\infty}^{0} dt'\Theta''(t-t')\varrho_0(t') = 0 \tag{4.26}$$

and the condition $\varrho_0(0) = 1$ define $\varrho_0(t)$ uniquely.

Although the kernels (4.23) and (4.25) have quite a different appearance, their Fourier transforms turn out to be closely related, as are the functions $\varrho_0(t)$ defined by Eqs. (4.24) and (4.26). Indeed, as shown in Appendix D,

$$\varrho_0(t)|_{\text{Lieb-Liniger}} = \varrho_0(-t)|_{\text{quantum Toda}}. \tag{4.27}$$

In view of Eqs. (4.17) and (4.21), Eq. (4.27) translates to the relation

$$E(S)|_{\text{Lieb-Liniger}} = E(-S)|_{\text{quantum Toda}}, \tag{4.28}$$

and Eq. (4.16) yields

$$e_{\pm}(s)|_{\text{Lieb-Liniger}} = -e_{\mp}(s)|_{\text{quantum Toda}}, \tag{4.29}$$

in agreement with the results of Secs. II and III.

C. Evaluation of the crossover functions

Equation (4.24) is of Wiener-Hopf type and can be solved analytically; see Appendix C. The solution satisfying $\varrho_0(0) = 1$ can be written as

$$\varrho_0(t) = \frac{1}{\pi\sqrt{2\pi}}\int_0^{\infty}\frac{dz}{z^{1/2}}\sin(2\pi z)\Gamma(z)\,e^{-z(\ln z - 1 + 2\pi t)} \tag{4.30a}$$

at $t > 0$ and

$$\varrho_0(t) = \frac{1}{\pi\sqrt{2\pi}}\fint_0^{\infty}\frac{dz}{z^{3/2}}\left[1 - \frac{\pi e^{z(\ln z - 1 + 2\pi t)}}{\tan(\pi z)\Gamma(z)}\right] \tag{4.30b}$$

at $t < 0$. Simple poles at integer z in the integrand of Eq. (4.30b) are understood in the Cauchy principal value sense. The function $\varrho_0(t)$ is plotted in Fig. 1.

As expected for a solution of an integral equation with a nonsingular kernel [see Eqs. (4.23) and (4.24)], $\varrho_0(t)$ is an analytic function. It is easy to check that $\varrho_0(t) > 0$ and $d\varrho_0(t)/dt < 0$. The first of these inequalities implies that the

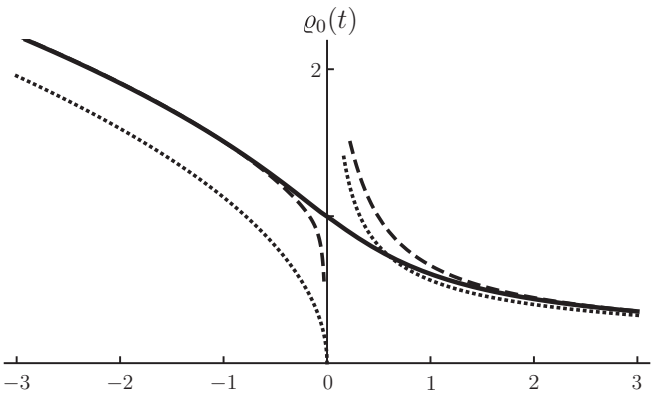

FIG. 1. The function $\varrho_0(t)$ for the Lieb-Liniger model. The solid line is a plot of the exact result given by Eqs. (4.30). The dotted lines represent Eq. (4.19), applicable at $|t| \gg 1$, i.e., in the classical regime. The dashed lines correspond to Eqs. (4.31), which include the leading quantum corrections.

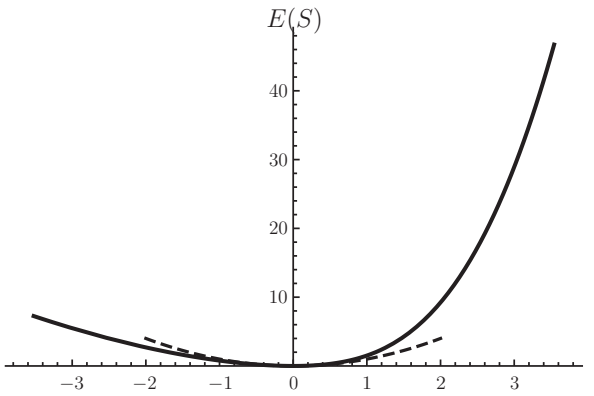

FIG. 2. The function $E(S)$ for the Lieb-Liniger model. The solid line is a plot of the exact result obtained by substituting Eqs. (4.30) into Eqs. (4.17) and (4.21). The dashed line is a plot of $E(S) = S^2$, applicable in the quantum regime $|S| \ll 1$ [see Eq. (4.36)].

function $E(S)$ defined by Eqs. (4.17) and (4.21) is analytic. This function is plotted in Fig. 2. It satisfies $E''(S) > 0$ at all S and $E(0) = E'(0) = 0$. Accordingly, the crossover functions $e_{\pm}(s)$ [see Eq. (4.16)] and their derivatives $e_{\pm}'(s)$ vanish at $s = 0$, whereas $e_{+}'(s) > 0$ and $e_{-}'(s) < 0$ at finite s.

The asymptotes of the crossover functions in the classical ($s \gg 1$) and quantum ($s \ll 1$) regimes can be found analytically. At large $|t|$, Eqs. (4.30) yield

$$\varrho_0(t)|_{t\gg 1} = (\pi t)^{-1/2}\left[1 + \frac{\ln(8\pi t) - 1}{4\pi t} + \cdots\right], \tag{4.31a}$$

$$\varrho_0(t)|_{-t\gg 1} = \left|\frac{4t}{\pi}\right|^{1/2}\left[1 + \frac{\ln|8\pi t| + 1}{|4\pi t|} + \cdots\right], \tag{4.31b}$$

in agreement with Eq. (4.19). Substitution into Eqs. (4.17) and (4.21) then gives

$$E(S)|_{S\gg 1} = S^3 + \frac{2}{3}S + \cdots, \tag{4.32a}$$

$$E(S)|_{-S\gg 1} = \frac{3}{5}\left(\frac{2\pi}{3}\right)^{2/3}|S|^{5/3} - \frac{2}{9}|S| + \cdots. \tag{4.32b}$$

Interestingly, the logarithmic terms, dominating the corrections to $\varrho_0(t)$ in Eqs. (4.31), do not contribute to the expansions (4.32).

Taking into account Eqs. (4.16) and (4.29), we obtain the asymptotes of the crossover functions in the classical regime $s \gg 1$,

$$e_{+}(s) = s^3 + \frac{2}{3}s + \cdots, \tag{4.33a}$$

$$e_{-}(s) = -\frac{3}{5}\left(\frac{2\pi}{3}\right)^{2/3}s^{5/3} + \frac{2}{9}s + \cdots \tag{4.33b}$$

for the Lieb-Liniger model, and

$$e_{+}(s) = \frac{3}{5}\left(\frac{2\pi}{3}\right)^{2/3}s^{5/3} - \frac{2}{9}s + \cdots, \tag{4.34a}$$

$$e_{-}(s) = -s^3 - \frac{2}{3}s + \cdots \tag{4.34b}$$

for the quantum Toda model. The first terms on the right-hand sides of Eqs. (4.33) and (4.34) can be deduced from the solutions of the classical equation of motion; see Eqs. (2.20) and (2.21). The second terms in Eqs. (4.33) and (4.34) represent the leading quantum corrections.

At small $|t|$, the function $\varrho_0(t)$ can be expanded in Taylor series. The first two terms of the expansion read

$$\varrho_0(t)|_{|t|\ll 1} = 1 - \pi t/6 + \cdots \tag{4.35}$$

(see Appendix C), and Eqs. (4.17) and (4.21) result in

$$E(S)|_{|S|\ll 1} = S^2 + \tfrac{1}{3}S^3 + \cdots, \tag{4.36}$$

which yields

$$e_\pm(s) = \pm s^2 + \tfrac{1}{3}s^3 + \cdots \tag{4.37}$$

for the Lieb-Liniger model and

$$e_\pm(s) = \pm s^2 - \tfrac{1}{3}s^3 + \cdots \tag{4.38}$$

for the quantum Toda model in the quantum regime $s \ll 1$. The leading contributions in Eqs. (4.37) and (4.38) correspond to the particle and hole excitations of a gas of free fermions with a quadratic dispersion relation; see Eq. (2.26).

V. DISCUSSION

The regime in which the interaction between particles dominates the energy of a quantum system is often referred to as classical. Indeed, many properties of a quantum system in this regime can be understood by solving the corresponding classical equations of motion. Paradigmatic examples of one-dimensional systems exhibiting such semiclassical behavior are identical bosons with a weak short-range repulsion and identical particles, either bosons or fermions, with a strong long-range repulsion. Despite the obvious difference between these two families of systems, it can be shown that their low-energy excitations admit a universal description in terms of the quantized version of the so-called first Hamiltonian structure [2] of the KdV equation. This observation implies, in particular, that the spectra of elementary excitations for the members of the two families are related to that of the quantum KdV model (2.10), and, therefore, to each other; see Eq. (3.2).

The relevant classical equation of motion is the celebrated KdV equation (2.1). This equation has two physically and mathematically distinct types of solutions: the delocalized periodic waves, corresponding to phonons in quantum systems, and the solitons. The classical solutions translate to power-law excitation spectra characterized by different exponents for phonons and solitons; see Eqs. (2.19)–(2.21). Importantly, in quantum systems these two excitation branches are not independent, and their spectra can be viewed as analytical continuations of one another [see Eqs. (4.15) and (4.16)], with the classical expressions (2.20) and (2.21) serving as high-energy asymptotes.

At the lowest energies, the classical treatment inevitably breaks down. Instead, the system is best described in terms of weakly interacting fermions with a quadratic spectrum [5,31]. These effective fermions can be used to characterize the elementary excitations in the classical regime as well. Indeed, as discussed in Sec. II, the bright (dark) solitons carry a macroscopic number of fermionic particles (holes). With the decrease of the soliton's energy, this number decreases, becoming unity when the bright (dark) soliton reaches its ultimate quantum fate of being demoted to a single-particle (hole) excitation of the effective Fermi gas.

In this paper, we considered in detail the integrable members of the two families of systems mentioned above, namely the Lieb-Liniger model (3.3) and the quantum Toda model (3.25). The key advantage of working with integrable models is that their excitation spectra can be found analytically, yielding explicit expressions valid throughout the classical-to-quantum crossover; see Sec. IV. The spectra we found satisfy Eqs. (4.15) and (4.29), as expected for models with quantum KdV-type low-energy behavior (see Sec. III).

Our results can be reformulated in terms of the exact spectra of the elementary excitations of the quantum KdV model defined by Eqs. (2.7), (2.9), and (2.10),

$$\varepsilon_\pm(p) = \pm\varepsilon_* E(\mp p/p_*). \tag{5.1}$$

Here $\varepsilon_\pm$ and p are eigenvalues of the operators $H_{\rm KdV}$ [see Eq. (2.10)] and P [see Eq. (2.9)], and ε_* and p_* are the energy and momentum scales expressed via the parameters m_* and a_* of $H_{\rm KdV}$ according to Eq. (2.18). The dimensionless function $E(S)$ in Eq. (5.1) is defined parametrically by Eqs. (4.17), (4.21), and (4.30). This function is plotted in Fig. 2, and its asymptotes are given in Eqs. (4.32) and (4.36). Because the quantum KdV Hamiltonian (2.10) is chiral, the two excitation branches $\varepsilon_\pm(p)$ coincide with the bounds on the excitation energy ε at a given momentum p: $\varepsilon_-(p) \leqslant \varepsilon \leqslant \varepsilon_+(p)$.

Finally, we note that the derivation of the low-energy quantum KdV theories for the Lieb-Liniger and the quantum Toda models in Sec. III does not rely on their integrability and can be readily adapted for generic (i.e., nonintegrable) systems [9]. In such systems, $\varepsilon_+(p)$ excitation mode no longer represents the exact eigenstate and, therefore, has a finite lifetime even at zero temperature [5,9,42–45]. However, the resulting inelastic broadening is parametrically small near the classical limit [9,45]. Therefore, we expect our results for the excitation spectra to be applicable to all quantum one-dimensional systems with a classical limit described by the KdV equation.

ACKNOWLEDGMENTS

We benefited from discussions with A. G. Abanov. This work was supported by the US Department of Energy, Office of Science, Materials Sciences and Engineering Division. We are grateful to the Aspen Center for Physics (NSF Grant No. PHYS-1066293) for hospitality.

APPENDIX A: CLASSICAL REGIME FROM THE BETHE ANSATZ

In this Appendix, we review asymptotic solutions [12,13,18,22] of the Bethe ansatz equations (4.3) and (4.4) at $q_*/q_0 \sim \zeta$ approaching zero. Here $q_* = c$ for the Lieb-Liniger model and $q_* = 2/a_0$ for the hyperbolic Calogero-Sutherland model in the Toda limit.

It is convenient to work with dimensionless rapidities $k = q/q_*$. After such rescaling, the Lieb equation (4.3) and the Yang-Yang equation (4.4) become

$$\rho(k) + \frac{1}{2\pi}\int_{-k_0}^{k_0} dk'\Theta'(k-k')\rho(k') = \frac{1}{2\pi}, \tag{A1a}$$

$$\sigma(k) + \frac{1}{2\pi}\int_{-k_0}^{k_0} dk'\Theta'(k-k')\sigma(k') = \frac{\hbar^2 q_*}{m}k. \tag{A1b}$$

The dimensionless Fermi rapidity $k_0 = q_0/q_*$ is to be determined self-consistently from the normalization condition

$$\int_{-k_0}^{k_0} dk\,\rho(k) = \frac{n_0}{q_*}, \tag{A2}$$

see Eq. (4.2). In the regimes we consider, $k_0 \sim 1/\zeta \gg 1$.

We are interested in the behavior of the functions $\rho(k)$ and $\sigma(k)$ at k in the range $||k| - k_0| \gg 1$. The momenta $p(k)$ corresponding to such k satisfy $p(k) \gg p_*$, i.e., they belong to the classical regime in the excitation spectra.

1. Lieb-Liniger model

For $k_0 \gg 1$, the integrals on the left-hand sides of Eqs. (A1) are dominated by k' satisfying $k_0 - |k'| \gg 1$. Moreover, it is natural to assume that both at $k_0 - |k| \gg 1$ and at $|k| - k_0 \gg 1$ the functions $\rho(k)$ and $\sigma(k)$ vary with k on the scale of order k_0 as no other scale is available. Therefore, in order to find $\rho(k)$ and $\sigma(k)$ at $||k| - k_0| \gg 1$, it is sufficient to replace the two-particle scattering phase shift $\Theta(k) = -2\arctan k$ [see Eq. (4.7)] in Eqs. (A1) by its asymptote

$$\widetilde{\Theta}(k) = \Theta(k)|_{|k|\gg 1} = -\pi\,\mathrm{sgn}(k) + \frac{2}{k}. \tag{A3}$$

With this approximation, Eq. (A1a) simplifies to

$$\theta(|k| - k_0)\rho(k) + \frac{1}{\pi}\frac{d}{dk}\fint_{-k_0}^{k_0} dk'\frac{\rho(k')}{k-k'} = \frac{1}{2\pi}, \tag{A4}$$

with the pole in the integrand treated as the Cauchy principal value.

Unlike the exact phase shift $\Theta(k)$, the approximate phase shift $\widetilde{\Theta}(k)$ has a singularity at $k = 0$. This singularity translates to nonanalyticities at $k \to \pm k_0$ in the solutions of the approximate Lieb equation (A4). In fact, the interior of the interval $|k| < k_0$ does not enter Eq. (A4) on an equal footing with its exterior: Eq. (A4) can be viewed both as an equation for $\rho(k)$ in the interior and as a prescription for extending the solution from the interior to the exterior.

Another difficulty that stems from the singular behavior of $\widetilde{\Theta}(k)$ is that Eq. (A4) does not determine $\rho(k)$ at $|k| < k_0$ uniquely: if $\rho(k)$ is a solution, then $\rho + \delta\rho$ with $\delta\rho \propto (k_0^2 - k^2)^{-1/2}$ is a solution as well. The ambiguity can be removed by imposing appropriate boundary conditions. For $\zeta \to 0$, such conditions read [13]

$$\rho(k)|_{k=\pm(k_0-0)} = 0. \tag{A5}$$

The conditions (A5) are justified by the observation that the exact density $\rho(k)$ near the boundaries of the interval $|k| < k_0$ is parametrically smaller than that in its interior. Indeed, with the help of Eq. (A4), $\rho(k)$ at $k_0 - |k| \gg 1$ is estimated as $\rho(k) \sim \rho(0) \sim k_0$. Substituting this estimate into Eq. (A2), we find $k_0 \sim \gamma^{-1/2}$. On the other hand, at $k_0 - |k| \lesssim 1$ [recall that such k are not handled properly by the approximate equation (A4)] we have $\rho(k) \sim \rho_0$, where $\rho_0 \sim K^{1/2} \sim \gamma^{-1/4}$ is the exact value of $\rho(k)$ at the Fermi rapidity; see Eqs. (4.6) and (3.11). Thus, the ratio of $\rho(k)$ near the boundaries to that in the interior is indeed small, of order $\gamma^{1/4} \sim \zeta^{1/2}$ [see Eqs. (3.11) and (3.23)].

The solution of Eq. (A4) subject to the conditions (A5) is unique and reads [13,22]

$$\rho(k) = \frac{1}{2\pi} \times \begin{cases} \left(k_0^2 - k^2\right)^{1/2}, & |k| < k_0, \\ \mathrm{sgn}(k)\frac{d}{dk}\left(k^2 - k_0^2\right)^{1/2}, & |k| > k_0. \end{cases} \tag{A6}$$

Substituting Eq. (A6) into Eq. (A2) and taking into account Eqs. (3.11) and (3.23), we obtain

$$k_0 = \frac{2}{\sqrt{\gamma}} = \frac{2K}{\pi} = \frac{9}{4\pi\zeta} \tag{A7}$$

for the dimensionless Fermi rapidity, in agreement with the above estimate.

We now focus on the realm of the long-wavelength excitations, where the universal KdV description is applicable. For such excitations k is close to k_0, and Eq. (A6) can be expanded in powers of $|k - k_0|/k_0$, leading to

$$\rho(k) = \frac{k_0}{\pi}\left[\left(\frac{k_0-k}{2k_0}\right)^{1/2} - \frac{1}{2}\left(\frac{k_0-k}{2k_0}\right)^{3/2} + \cdots\right] \tag{A8a}$$

at $k < k_0$ and

$$\rho(k) = \frac{1}{4\pi}\left[\left(\frac{k-k_0}{2k_0}\right)^{-1/2} + \frac{3}{2}\left(\frac{k-k_0}{2k_0}\right)^{1/2} + \cdots\right] \tag{A8b}$$

at $k > k_0$. Changing the variable to $t = k - k_0$ [see Eq. (4.12)] and taking into account Eqs. (4.6), (4.13), and (A7), we rewrite Eqs. (A8) in a more compact form as

$$\varrho(t) = \frac{\rho(t)}{\rho_0} = \varrho_0(t) + \frac{\pi\zeta}{6}\int_0^t dt'\varrho_0(t') + \cdots, \tag{A9}$$

where

$$\varrho_0(t) = \theta(-t)|4t/\pi|^{1/2} + \theta(t)(\pi t)^{-1/2}. \tag{A10}$$

Equation (A9) represents the expansion in small $\zeta t \sim (k - k_0)/k_0$ of the dominant at $\zeta \to 0$ and fixed ζt contribution to the normalized density ϱ. Alternatively, Eq. (A9) can be interpreted as an asymptotic expansion in small ζ of $\varrho(t)$ evaluated at fixed t, with t-dependent expansion coefficients found at $|t| \gg 1$; cf. Ref. [46]. Although in such an interpretation Eqs. (A9) and (A10) are applicable only at large $|t|$, it is reassuring that at $|t| \sim 1$ they yield the correct estimate $\varrho_0(t) \sim 1$.

Analysis of the Yang-Yang equation (A1b) follows the same steps. Approximating $\Theta(k)$ in Eq. (A1b) by $\widetilde{\Theta}(k)$ [see Eq. (A3)] and taking into account Eq. (A7), we obtain the equation

$$\theta(|k| - k_0)\sigma(k) + \frac{1}{\pi}\frac{d}{dk}\fint_{-k_0}^{k_0} dk'\frac{\sigma(k')}{k-k'} = \frac{2\pi\hbar v k}{k_0}. \tag{A11}$$

As with Eq. (A4), Eq. (A11) does not define $\sigma(k)$ uniquely and must be augmented with appropriate boundary conditions at $k \to \pm k_0$. At $k_0 - |k| \gg 1$ we have $|\sigma(k)| \sim \hbar v k_0 \sim \hbar v\gamma^{-1/2}$, which for $\gamma \sim \zeta^2 \ll 1$ is parametrically larger than

$\sigma(k)$ at k approaching k_0,$\sigma(k) \sim \sigma_0 \sim \hbar v \gamma^{-1/4}$, see Eqs. (4.6) and (A7). This observation leads to the condition

$$\sigma(k)|_{k=\pm(k_0-0)} = 0, \tag{A12}$$

cf. Eq. (A5). The solution of Eq. (A11) satisfying the conditions (A12) is given by [22]

$$\sigma(k) = \frac{\hbar v}{3k_0} \times \begin{cases} -\frac{d}{dk}\left(k_0^2 - k^2\right)^{3/2}, & |k| < k_0, \\ \mathrm{sgn}(k)\frac{d^2}{dk^2}\left(k^2 - k_0^2\right)^{3/2}, & |k| > k_0. \end{cases} \tag{A13}$$

Expanding Eq. (A13) in $(k - k_0)/k_0 \sim \zeta t$ and taking into account Eqs. (4.6) and (4.13), we find

$$\varsigma(t) = \frac{\sigma(t)}{\sigma_0} = \varrho_0(t) + \frac{5\pi\zeta}{6}\int_0^t dt' \varrho_0(t') + \cdots \tag{A14}$$

with $\varrho_0(t)$ given by Eq. (A10). Similar to Eq. (A9), Eq. (A14) can be viewed as an asymptotic expansion in small ζ of the function $\varsigma(t)$ evaluated at fixed t such that $|t| \gg 1$, which corresponds to the classical regime in the excitation spectra. Substitution of Eqs. (A9) and (A14) into Eq. (4.18b) yields Eq. (4.21).

2. Quantum Toda model

Instead of attacking the quantum Toda model directly, we consider the hyperbolic Calogero-Sutherland model (3.29) in the Toda limit defined by Eqs. (3.28) and (3.32). As shown in Refs. [12,18] and confirmed below, under these conditions the dimensionless Fermi rapidity k_0 in the Bethe ansatz equations (A1) satisfies

$$1 \ll k_0 \ll \lambda. \tag{A15}$$

Accordingly, for $|k| \sim k_0 \ll \lambda$ the two-particle phase shift

$$\Theta(k) = 2\,\mathrm{Im}[\ln\Gamma(\lambda + ik) - \ln\Gamma(1 + ik)] \tag{A16}$$

[see Eq. (4.8)] can be replaced with

$$\Theta(k)|_{|k|\ll\lambda} = 2k\ln\lambda - 2\,\mathrm{Im}\ln\Gamma(1 + ik). \tag{A17}$$

This approximation ignores the existence of the regime $|k| \gg \lambda$, absent in the true quantum Toda model [20], but it is adequate for our purposes. On the other hand, similar to the Lieb-Liniger model, the dominant contribution to the integrals on the left-hand sides of Eqs. (A1) comes from k' satisfying $k_0 - |k'| \gg 1$. Thus, in order to find $\rho(k)$ and $\sigma(k)$ at k in the range $||k| - k_0| \gg 1$, the phase shift can be further approximated by

$$\widetilde{\Theta}(k) = \Theta(k)|_{1\ll|k|\ll\lambda} = 2k(\ln|\lambda/k| + 1). \tag{A18}$$

The Lieb equation (A1a) then assumes the form [12,18]

$$\rho(k) + \frac{1}{\pi}\int_{-k_0}^{k_0} dk' \ln\left|\frac{\lambda}{k - k'}\right|\rho(k') = \frac{1}{2\pi}. \tag{A19}$$

Similar to Eq. (A4) for the Lieb-Liniger model, Eq. (A19) serves simultaneously as an equation for $\rho(k)$ in the interior of the interval $|k| < k_0$, and as a prescription for extending $\rho(k)$ from the interior to the exterior. Moreover, at $|k| < k_0$ the first term on the left-hand side of Eq. (A19) can be neglected [12,18]. Indeed, at $k_0 - |k| \gg 1$ this term is of order $\rho(k) \sim \rho(0)$, whereas the second term is parametrically larger, of order $k_0\ln(\lambda/k_0)\rho(0) \gg \rho(0)$.

With these approximations, the Lieb equation can be solved exactly [12,18]. The solution reads

$$\rho(k) = \frac{1}{2\pi\ln(2\lambda/k_0)} \times \begin{cases} \left(k_0^2 - k^2\right)^{-1/2}, & |k| < k_0, \\ \mathrm{arccosh}(k/k_0), & |k| > k_0. \end{cases} \tag{A20}$$

The normalization condition (A2) and Eqs. (3.39) and (3.43) then yield

$$k_0 = 2\lambda e^{-\alpha} = \frac{\pi}{2\alpha^2 K} = \frac{3}{4\pi\zeta} \tag{A21}$$

for the dimensionless Fermi rapidity. Since $\lambda \gg e^{\alpha} \gg 1$ [see Eqs. (3.28) and (3.32)], k_0 indeed satisfies the inequalities (A15). In the same approximation, $\Theta(k) \approx \widetilde{\Theta}(k)$ [see Eq. (A18)], the Yang-Yang equation (A1b) yields [12,18]

$$\sigma(k) = \frac{\hbar v}{\alpha k_0} \times \begin{cases} -\frac{d}{dk}\left(k_0^2 - k^2\right)^{1/2}, & |k| < k_0, \\ \mathrm{sgn}(k)\left(k^2 - k_0^2\right)^{1/2}, & |k| > k_0. \end{cases} \tag{A22}$$

Focusing on the long-wavelength excitations, we expand Eqs. (A20) and (A22) in powers of small $(k - k_0)/k_0 = 4\pi\zeta t/3$. With Eqs. (4.6) and (4.13) taken into account, the first two terms of these expansions can be written as

$$\varrho(t) = \varrho_0(t) - \frac{\pi\zeta}{6}\int_0^t dt' \varrho_0(t') + \cdots, \tag{A23a}$$

$$\varsigma(t) = \varrho_0(t) + \frac{\pi\zeta}{2}\int_0^t dt' \varrho_0(t') + \cdots \tag{A23b}$$

with $\varrho_0(t)$ given by

$$\varrho_0(t) = \theta(-t)|\pi t|^{-1/2} + \theta(t)(4t/\pi)^{1/2}. \tag{A24}$$

Similar to their Lieb-Liniger model counterparts (A9) and (A14), Eqs. (A23) can be interpreted as asymptotic expansions in small ζ of the functions $\varrho(t)$ and $\varsigma(t)$ evaluated at fixed large t. Although the numerical coefficients in front of the second terms on the right-hand sides of Eqs. (A23) differ from those in Eqs. (A9) and (A14), the difference does not affect the form of the function $\eta_0(t)$ [see Eq. (4.18b)], which is again given by Eq. (4.21).

APPENDIX B: BEYOND THE CLASSICAL REGIME

Equation (4.21) can be obtained by substituting $\varrho(t)$ and $\varsigma(t)$ in the form of Eqs. (A9) and (A14) for the Lieb-Liniger model and Eqs. (A23) for the quantum Toda model into Eq. (4.18b). However, such a derivation is valid only at $|t| \gg 1$, i.e., in the classical regime in the excitation spectra, whereas we are interested in $|t| \sim 1$, which corresponds to the classical-to-quantum crossover. It turns out that relaxing the restriction $|t| \gg 1$ requires merely a replacement of the functions $\varrho_0(t)$ in Eqs. (A9), (A14), (A23), and (4.21) with the exact solutions of Eqs. (4.24) or (4.26). In this Appendix, we derive such a generalization of the expansion (A9) for the Lieb-Liniger model. Generalizations of Eqs. (A14) and (A23) can be obtained in a similar manner.

It is convenient to write the Lieb equation (4.22) as

$$\mathcal{L}_{2k_0}[\varrho] = \frac{1}{2\pi\rho_0}. \tag{B1}$$

Here $k_0 \sim 1/\zeta$, $\rho_0 \sim \zeta^{-1/2}$ [see Eqs. (4.6) and (A7)], and the functional $\mathcal{L}_\tau$ is defined by

$$\mathcal{L}_\tau[f] = f(t) + \frac{1}{2\pi}\int_{-\tau}^{0} dt' \Theta'(t-t') f(t'), \tag{B2}$$

where $\Theta(t) = -2\arctan t$. The solution of Eq. (B1) can be viewed as a function of two variables, t and ζ. We are interested in the behavior of $\varrho(t,\zeta)$ at arbitrary t and small $\zeta \ll \min\{1, |t|^{-1}\}$.

Replacement of the phase shift $\Theta(t)$ in Eq. (B2) with $\widetilde{\Theta}(t)$ given by Eq. (A3) leads to the approximate Lieb equation

$$\widetilde{\mathcal{L}}_{2k_0}[\widetilde{\varrho}\,] = \frac{1}{2\pi\rho_0}, \tag{B3}$$

which, unlike Eq. (B1), is exactly solvable. To avoid confusion, in this Appendix we use a tilde to distinguish the exact solution $\widetilde{\varrho}(t,\zeta)$ of the approximate Lieb equation (B3) from the solution $\rho(t,\zeta)$ of the exact Lieb equation (B1). At $\zeta|t| \ll 1$, the function $\widetilde{\varrho}(\zeta,t)$ can be expanded as

$$\widetilde{\varrho}(t,\zeta) = \widetilde{\varrho}_0(t) + \frac{\pi\zeta}{6}\widetilde{\varrho}_1(t) + \cdots \tag{B4}$$

with $\widetilde{\varrho}_1(t) = \int_0^t dt' \widetilde{\varrho}_0(t')$ [see Eq. (A9)]. The function $\widetilde{\varrho}_0(t)$ in Eq. (B4) satisfies the equation

$$\widetilde{\mathcal{L}}_\infty[\widetilde{\varrho}_0] = 0 \tag{B5}$$

and is given by $\widetilde{\varrho}_0(t) = \theta(-t)|4t/\pi|^{1/2} + \theta(t)(\pi t)^{-1/2}$ [see Eq. (A10)].

We seek the solution of Eq. (B1) in the form of an expansion inspired by Eq. (B4),

$$\varrho(t,\zeta) = \varrho_0(t) + \frac{\pi\zeta}{6}\varrho_1(t) + \cdots, \tag{B6}$$

where the functions $\varrho_0(t)$ and $\varrho_1(t)$ are independent of ζ. Since $\varrho(0,\zeta) = 1$ for any ζ, these functions satisfy

$$\varrho_0(0) = 1, \quad \varrho_1(0) = 0. \tag{B7}$$

On the other hand, we expect the functions $\varrho(t,\zeta)$ and $\widetilde{\varrho}(t,\zeta)$ to match at $1 \ll |t| \ll 1/\zeta$ in every order in ζ. This leads to the relations

$$\lim_{|t|\to\infty} \frac{\varrho_0(t)}{\widetilde{\varrho}_0(t)} = 1, \quad \lim_{|t|\to\infty} \frac{\varrho_1(t)}{\widetilde{\varrho}_1(t)} = 1, \tag{B8}$$

so that $\varrho_1'(t) = d\varrho_1(t)/dt$ satisfies

$$\lim_{|t|\to\infty} \frac{\varrho_1'(t)}{\widetilde{\varrho}_0(t)} = 1, \tag{B9}$$

where we used $\widetilde{\varrho}_1'(t) = \widetilde{\varrho}_0(t)$.

Formally, the right-hand side of Eq. (B6) represents an asymptotic expansion of $\varrho(t,\zeta)$ in small ζ evaluated at fixed t. The expansion is applicable as long as the second term is small compared with the first one. With Eqs. (B7) and (B8) taken into account, this yields the condition $\zeta \ll \min\{1, |t|^{-1}\}$ on ζ, which translates to $|t| \ll 1/\zeta$ for t. Taking advantage of this inequality, we introduce the intermediate scale τ satisfying

$$\max\{1, |t|\} \ll \tau \ll 1/\zeta, \tag{B10}$$

break the integral in $\int_{-2k_0}^{0} dt' \Theta'(t-t')\varrho(t')$ in two, $\int_{-2k_0}^{0} dt'[\cdots] = \int_{-\tau}^{0} dt'[\cdots] + \int_{-2k_0}^{-\tau} dt'[\cdots]$, and replace Θ and ρ in the second integral here with $\widetilde{\Theta}$ and $\widetilde{\varrho}$. (The relative error of such an approximation is of order $1/\tau \ll 1$.) With the help of Eqs. (B1)–(B3), we obtain the equation

$$\mathcal{L}_\tau[\varrho] = \widetilde{\mathcal{L}}_\tau[\widetilde{\varrho}\,]. \tag{B11}$$

The functions $\varrho_0(t)$ and $\varrho_1(t)$ in Eq. (B6) can now be deduced by replacing $\widetilde{\varrho}$ and ϱ in Eq. (B11) with the expansions (B4) and (B6), respectively, and considering the behavior of the resulting equation at small ζ and large τ. For the equation to hold at large, but still finite τ and arbitrarily small $\zeta \ll 1/\tau$ [see Eq. (B10)], it must be satisfied in every order in ζ separately. This observation leads to the equations

$$\mathcal{L}_\tau[\varrho_0] = \widetilde{\mathcal{L}}_\tau[\widetilde{\varrho}_0], \tag{B12a}$$

$$\mathcal{L}_\tau[\varrho_1] = \widetilde{\mathcal{L}}_\tau[\widetilde{\varrho}_1]. \tag{B12b}$$

Differentiating these equations with respect to τ, we recover the relations (B8) and (B9).

In the limit $\tau \to \infty$, Eq. (B12a) yields

$$\mathcal{L}_\infty[\varrho_0] = 0, \tag{B13}$$

where we took into account Eq. (B5). Equation (B13) coincides with Eq. (4.24). The solution of this equation satisfying the condition $\varrho_0(0) = 1$ [see Eq. (B7)] is unique and behaves at large $|t|$ as prescribed by the first equation in (B8); see Sec. IV C and Appendix C.

Because the integrals in Eq. (B12b) diverge at $\tau \to \infty$, we first differentiate both sides of this equation with respect to t and integrate by parts using $\varrho_1(0) = \widetilde{\varrho}_1(-0) = 0$. Taking now the limit $\tau \to \infty$ and using Eq. (B5), we obtain the equation

$$\mathcal{L}_\infty[\varrho_1'] = 0. \tag{B14}$$

Its solution subject to the condition (B9) reads $\varrho_1'(t) = \varrho_0(t)$. Combining this result with the second equation in (B7), we finally arrive at

$$\varrho_1(t) = \int_0^t dt' \varrho_0(t'). \tag{B15}$$

By construction, Eq. (B6) with $\varrho_1(t)$ given by Eq. (B15) has the form of Eq. (A9). We have verified that Eqs. (B6) and (B15) with $\varrho_0(t)$ approximated by its asymptote (4.31b) are in agreement with the expansion derived by a different method in Ref. [46].

APPENDIX C: SOLUTION OF EQ. (4.24)

In this Appendix, we employ the Wiener-Hopf technique (see, e.g., Ref. [47]) to construct the solution of Eq. (4.24).

Substituting $\varrho_0(t)$ in the form

$$\varrho_0(t) = \varrho_+(t) + \varrho_-(t), \quad \varrho_\pm(t) = \theta(\pm t)\,\varrho_0(t) \tag{C1}$$

into Eq. (4.24), we obtain the equation

$$\varrho_+(t) + \int_{-\infty}^{\infty} dt' \mathcal{G}(t-t')\varrho_-(t') = 0 \tag{C2}$$

with

$$\mathcal{G}(t) = \delta(t) + \frac{\Theta'(t)}{2\pi} = \delta(t) - \frac{1}{\pi(1+t^2)}. \tag{C3}$$

Upon the Fourier transform, Eq. (C2) assumes the form

$$\varrho_+(\omega) + \mathcal{G}(\omega)\varrho_-(\omega) = 0. \tag{C4}$$

The functions

$$\varrho_\pm(\omega) = \int_{-\infty}^{\infty} dt\, e^{i\omega t}\varrho_\pm(t) \tag{C5}$$

in Eq. (C4) are analytic at $\pm \mathrm{Im}\,\omega \geqslant 0$. Their behavior at large $|\omega|$ is obtained by substituting $\varrho_0(t)$ in the form of the Taylor series $\varrho_0(t) = 1 + \varrho_0'(0)t + \cdots$ [recall that $\varrho_0(0) = 1$] into Eqs. (C1) and (C5), which yields

$$\varrho_\pm(\omega)|_{|\omega|\gg 1} = \pm\frac{i}{\omega}\left[1 + \varrho_0'(0)\frac{i}{\omega} + \cdots\right]. \tag{C6}$$

The kernel $\mathcal{G}(\omega)$ in Eq. (C4) is given by

$$\mathcal{G}(\omega) = \int_{-\infty}^{\infty} dt\, e^{i\omega t}\,\mathcal{G}(t) = 1 - e^{-|\omega|}. \tag{C7}$$

It can be factorized as

$$\mathcal{G}(\omega) = -\frac{F_+(\omega)}{F_-(\omega)} \tag{C8}$$

with

$$F_+(\omega) = \widetilde{\varrho}_+(\omega)f_+(\omega), \quad F_-(\omega) = \frac{\widetilde{\varrho}_-(\omega)}{f_-(\omega)}. \tag{C9}$$

Here

$$\widetilde{\varrho}_+(\omega) = \frac{e^{i\pi/4}}{(\omega + i0)^{1/2}}, \quad \widetilde{\varrho}_-(\omega) = \frac{e^{-3i\pi/4}}{(\omega - i0)^{3/2}} \tag{C10}$$

are Fourier transforms of $\widetilde{\varrho}_\pm(t) = \theta(\pm t)\widetilde{\varrho}_0(t)$, where $\widetilde{\varrho}_0(t)$ is the solution (A10) of the approximate Lieb equation (B5). The functions $\widetilde{\varrho}_\pm(\omega)$ are analytic in the complex plane with the branch cuts running from $\mp i0$ to $\mp i\infty$. The functions $f_\pm(\omega)$ in Eq. (C9) are given by

$$f_\pm(\omega) = \frac{\exp\left\{\mp i\frac{\omega}{2\pi}\left[\ln\left(\frac{\omega \pm i0}{2\pi}\right) - 1 \mp i\frac{\pi}{2}\right]\right\}}{\Gamma\left(1 \mp i\frac{\omega}{2\pi}\right)}, \tag{C11}$$

with the same branch cut structure. These functions approach 1 at $\omega \to 0$, whereas at large $|\omega|$ application of the Stirling formula gives the asymptotes

$$f_\pm(\omega)|_{|\omega|\gg 1} = \frac{e^{\pm i\pi/4}}{\sqrt{\omega}}\left(1 \mp \frac{i\pi}{6\omega} + \cdots\right). \tag{C12}$$

Because $\widetilde{\varrho}_\pm(\omega)$ and $f_\pm(\omega)$ have no singularities or zeros at $\pm \mathrm{Im}\,\omega \geqslant 0$, the functions $F_\pm(\omega)$ given by Eq. (C9) are analytic in these regions. Standard arguments [47] then show that the function

$$\mathcal{F}(\omega) = \frac{\varrho_+(\omega)}{F_+(\omega)} = \frac{\varrho_-(\omega)}{F_-(\omega)} \tag{C13}$$

is analytic in the entire complex plane. Using Eqs. (C6), (C9), (C10), and (C12), we find $\mathcal{F}(\omega)|_{|\omega|\to\infty} = 1$. Therefore, $\mathcal{F} = 1$ at all ω, and Eq. (C13) yields

$$\varrho_\pm(\omega) = F_\pm(\omega). \tag{C14}$$

At small ω, Eq. (C14) reduces to $\varrho_\pm(\omega)|_{|\omega|\ll 1} = \widetilde{\varrho}_\pm(\omega)$, hence at $|t| \gg 1$ the inverse Fourier transforms

$$\varrho_\pm(t) = \int_{-\infty}^{\infty}\frac{d\omega}{2\pi}\, e^{-i\omega t}\varrho_\pm(\omega) \tag{C15}$$

reproduce the classical asymptotes Eq. (4.19). At large ω, Eq. (C14) yields the expansion (C6) with

$$\varrho_0'(0) = -\pi/6, \tag{C16}$$

resulting in the Taylor series (4.35). At intermediate ω and t no further simplifications are possible. Instead, we deform the integration paths in Eq. (C15) to run along the respective branch cuts and change the integration variables to $z = \pm i\omega/2\pi$. Taking into account Eq. (C1), we arrive at Eqs. (4.30).

APPENDIX D: DERIVATION OF EQ. (4.27)

In this Appendix, we derive the relation (4.27) between the functions $\varrho_0(t)$ for the Lieb-Liniger model and for the quantum Toda model.

Substituting

$$\varrho_0(t) = \bar{\varrho}_0(-t) \tag{D1}$$

into Eq. (4.26) and using $\Theta''(t) = -\Theta''(-t)$ [see Eq. (4.25)], we obtain the equation

$$\bar{\varrho}_0'(t) + \frac{1}{2\pi}\int_0^{\infty} dt'\Theta''(t-t')\bar{\varrho}_0(t') = 0. \tag{D2}$$

Writing $\bar{\varrho}_0(t)$ as

$$\bar{\varrho}_0(t) = \bar{\varrho}_+(t) + \bar{\varrho}_-(t), \quad \bar{\varrho}_\pm(t) = \theta(\pm t)\bar{\varrho}_0(t) \tag{D3}$$

[cf. Eq. (C1)], and using the continuity of $\bar{\varrho}_0(t)$ at $t = 0$, we find

$$\bar{\varrho}_-'(t) + \int_{-\infty}^{\infty} dt'\bar{\mathcal{G}}'(t-t')\bar{\varrho}_+(t') = 0. \tag{D4}$$

Here

$$\overline{\mathcal{G}}(t) = \delta(t) - \frac{1}{\pi}\,\mathrm{Re}\,\psi(1 + it), \tag{D5}$$

where $\psi(z)$ is the digamma function. Fourier transform of Eq. (D5) reads

$$\overline{\mathcal{G}}(\omega) = \int_{-\infty}^{\infty} dt\, e^{i\omega t}\,\overline{\mathcal{G}}(t) = \frac{1}{1 - e^{-|\omega|}} = \frac{1}{\mathcal{G}(\omega)}, \tag{D6}$$

with $\mathcal{G}(\omega)$ given by Eq. (C7). With the help of Eq. (D6), the Fourier transform of Eq. (D4) can then be written as

$$\bar{\varrho}_+(\omega) + \mathcal{G}(\omega)\bar{\varrho}_-(\omega) = 0. \tag{D7}$$

Carrying out the inverse Fourier transform, we obtain

$$\bar{\varrho}_+(t) + \int_{-\infty}^{\infty} dt'\mathcal{G}(t-t')\bar{\varrho}_-(t') = 0, \tag{D8}$$

which is the same as Eq. (C2). The corresponding equation for $\bar{\varrho}_0(t)$ then coincides with Eq. (4.24) for the Lieb-Liniger model and is subject to the same constraint $\bar{\varrho}(0) = 1$ at $t = 0$. Therefore, $\bar{\varrho}_0(t)$ for the quantum Toda model is identical to $\varrho_0(t)$ for the Lieb-Liniger model, which leads to Eq. (4.27).

[1] D. J. Korteweg and G. De Vries, Philos. Mag. **39**, 422 (1895).

[2] S. Novikov, S. V. Manakov, L. P. Pitaevskii, and V. E. Zakharov, *Theory of Solitons: The Inverse Scattering Method* (Plenum, New York, 1984); A. C. Newell, *Solitons in Mathematics and Physics* (SIAM, Philadelphia, 1985).

[3] Y. S. Kivshar and B. A. Malomed, Rev. Mod. Phys. **61**, 763 (1989); E. A. Kuznetsov, A. M. Rubenchik, and V. E. Zakharov, Phys. Rep. **142**, 103 (1986).

[4] M. Khodas, A. Kamenev, and L. I. Glazman, Phys. Rev. A **78**, 053630 (2008).

[5] A. Imambekov, T. L. Schmidt, and L. I. Glazman, Rev. Mod. Phys. **84**, 1253 (2012).

[6] J. Lin, K. A. Matveev, and M. Pustilnik, Phys. Rev. Lett. **110**, 016401 (2013).

[7] G. E. Astrakharchik and L. P. Pitaevskii, Europhys. Lett. **102**, 30004 (2013).

[8] M. Pustilnik and K. A. Matveev, Phys. Rev. B **89**, 100504(R) (2014).

[9] M. Pustilnik and K. A. Matveev, Phys. Rev. B **91**, 165416 (2015).

[10] I. V. Protopopov, D. B. Gutman, M. Oldenburg, and A. D. Mirlin, Phys. Rev. B **89**, 161104(R) (2014).

[11] V. E. Korepin, N. M. Bogoliubov, and A. G. Izergin, *Quantum Inverse Scattering Method and Correlation Functions* (Cambridge University Press, Cambridge, 1997).

[12] B. Sutherland, *Beautiful Models* (World Scientific, Singapore, 2004).

[13] E. H. Lieb and W. Liniger, Phys. Rev. **130**, 1605 (1963); E. H. Lieb, *ibid.* **130**, 1616 (1963).

[14] C. N. Yang and C. P. Yang, J. Math. Phys. **10**, 1115 (1969).

[15] E. P. Gross, Nuovo Cimento **20**, 454 (1961); L. P. Pitaevskii, Sov. Phys. JETP **13**, 451 (1961).

[16] L. Pitaevskii and S. Stringari, *Bose-Einstein Condensation* (Oxford University Press, Oxford, 2003).

[17] T. Tsuzuki, J. Low Temp. Phys. **4**, 441 (1971).

[18] B. Sutherland, Rocky Mount. J. Math. **8**, 413 (1978).

[19] M. C. Gutzwiller, Ann. Phys. (N.Y.) **133**, 304 (1981).

[20] E. K. Sklyanin, Lect. Notes Phys. **226**, 196 (1985).

[21] M. Toda, Phys. Rep. **18**, 1 (1975); Prog. Theor. Phys. Suppl. **59**, 1 (1976); *Theory of Nonlinear Lattices*, 2nd ed. (Springer, Berlin, 1989).

[22] P. P. Kulish, S. V. Manakov, and L. D. Faddeev, Theor. Math. Phys. **28**, 615 (1976); M. Ishikawa and H. Takayama, J. Phys. Soc. Jpn. **49**, 1242 (1980).

[23] R. Sasaki and I. Yamanaka, Commun. Math. Phys. **108**, 691 (1987).

[24] A. K. Pogrebkov, Russ. Math. Surv. **58**, 1003 (2003); Theor. Math. Phys. **129**, 1586 (2001).

[25] V. V. Bazhanov, S. L. Lukyanov, and A. B. Zamolodchikov, Commun. Math. Phys. **177**, 381 (1996).

[26] B. A. Kupershmidt and P. Mathieu, Phys. Lett. B **227**, 245 (1989).

[27] R. Sasaki and I. Yamanaka, Adv. Stud. Pure Math. **16**, 271 (1988).

[28] P. Di Francesco, P. Mathieu, and D. Sénéchal, *Conformal Field Theory* (Springer, New York, 1999).

[29] M. Kulkarni and A. G. Abanov, Phys. Rev. A **86**, 033614 (2012).

[30] I. V. Protopopov, D. B. Gutman, P. Schmitteckert, and A. D. Mirlin, Phys. Rev. B **87**, 045112 (2013).

[31] A. V. Rozhkov, Eur. Phys. J. B **47**, 193 (2005).

[32] D. C. Mattis, J. Math. Phys. **15**, 609 (1974); A. Luther and I. Peschel, Phys. Rev. B **9**, 2911 (1974); S. Mandelstam, Phys. Rev. D **11**, 3026 (1975); A. K. Pogrebkov and V. N. Sushko, Theor. Math. Phys. **24**, 935 (1975).

[33] F. D. M. Haldane, J. Phys. C **14**, 2585 (1981).

[34] A. Hasegawa and M. Matsumoto, *Optical Solitons in Fibers* (Springer, Berlin, 2003); Y. S. Kivshar and G. P. Agrawal, *Optical Solitons: From Fibers to Photonic Crystals* (Academic, San Diego, 2003).

[35] V. N. Popov, Theor. Math. Phys. **11**, 565 (1972).

[36] F. D. M. Haldane, Phys. Rev. Lett. **47**, 1840 (1981).

[37] K. B. Efetov and A. I. Larkin, Sov. Phys. JETP **42**, 390 (1975).

[38] R. G. Pereira, J. Sirker, J.-S. Caux, R. Hagemans, J. M. Maillet, S. R. White, and I. Affleck, Phys. Rev. Lett. **96**, 257202 (2006); J. Stat. Mech. (2007) P08022.

[39] F. Calogero, O. Ragnisco, and C. Marchioro, Lett. Nuovo Cimento **13**, 383 (1975); F. Calogero, *ibid.* **16**, 22 (1976).

[40] L. D. Landau and E. M. Lifshitz, *Fluid Mechanics* (Butterworth-Heinemann, Oxford, 1987).

[41] K. A. Matveev and A. V. Andreev, Phys. Rev. B **86**, 045136 (2012); **85**, 041102(R) (2012).

[42] M. Khodas, M. Pustilnik, A. Kamenev, and L. I. Glazman, Phys. Rev. B **76**, 155402 (2007).

[43] K. A. Matveev and A. Furusaki, Phys. Rev. Lett. **111**, 256401 (2013).

[44] S. Tan, M. Pustilnik, and L. I. Glazman, Phys. Rev. Lett. **105**, 090404 (2010); I. E. Mazets, T. Schumm, and J. Schmiedmayer, *ibid.* **100**, 210403 (2008).

[45] Z. Ristivojevic and K. A. Matveev, Phys. Rev. B **89**, 180507 (2014).

[46] V. N. Popov, Theor. Math. Phys. **30**, 222 (1977).

[47] P. M. Morse and H. Feshbach, *Methods of Theoretical Physics, Part I* (McGraw-Hill, New York, 1953); B. Noble, *Methods Based on the Wiener-Hopf Technique for the Solution of Partial Differential Equations* (Pergamon, New York, 1958).